ISBN: 978-3-95450-132-8 doi:10.18429/JACoW-IPAC2014-WEPRO019

COMPARISON OF THE NSLS-II LINAC MODEL TO MEASUREMENTS*

R. P. Fliller III#, BNL, Upton, NY 11973

Abstract

The NSLS-II linac and associated transport lines were successfully installed and commissioned in the spring of 2012 and was restarted for booster commissioning in the fall of 2013. Various beam measurements were performed to ensure that the linac met specifications and would be a suitable injector for the NSLS-II booster. In this paper we discuss the outcomes of these measurements and compare them to the model of the NSLS-II linac.

INTRODUCTION

The NSLS-II linac was commissioned in the spring of 2012 and operated as an injector during booster and storage ring commissioning starting in the fall of 2013. In the interim, the modelling of the linac has progressed. In this paper we discuss the model of the NSLS-II linac and compare it measurements performed in the linac during booster and storage ring commissioning.

LINAC OVERVIEW

The NSLS-II linac was a turnkey procurement for RI Research Instruments Gmbh. It consists of a 90 kV electron gun, a 500 MHz subharmonic prebuncher, a 3 GHz prebuncher, a 3 GHz traveling wave buncher cavity, and four 3 GHz 5.2m accelerating sections. Solenoidal focusing is used in the low energy section of the linac, with quadrupole triplets between the accelerating sections. Various diagnostics are available in the linac and transport line for measurement. Details are given in other papers. [1,2] Figure 1 shows an overview of the linac and diagnostic transport line.

*This manuscript has been authored by Brookhaven Science Associates, LLC under Contract No. DE-AC02-98CH10886 with the U.S. Department of Energy.
#rfliller@bnl.gov

MODEL CONSTRUCTION

The linac is modelled using PARMELA. The model has been modified from the vendor supplied model so as to be as close to the as built and as run linac as possible. Where not possible to compare directly to as built conditions, such as the initial conditions at the cathode, beam measurements and first principles are used to reconstruct those conditions as close as possible.

The longitudinal location of all accelerator components within the model has been compared to its survey locations. Transverse misalignments of the various components have not been included within the model.

The cathode is an EIMAC YU-171 gridded thermionic cathode. It has an area of 1cm^2. Discussions with the cathode manufacturer revealed that the heater is a small solenoid internal to ceramic substrate. [3] The coil is wound so as not to cancel the fields produced by it, and the coil is smaller than the emitting surface of the cathode. The magnetic field on the cathode then has flux lines exiting the center of the cathode and returning near the edges of the cathode. A magnetic field on the cathode will produce canonical angular momentum, which is an x-y' coupling in the electron beam. [4] This will produce an x-y coupling at the end of the linac.

The divergence of the electron beam is determined by the cathode grid spacing and the voltages used to pulse it. Using the formalism of developed in Reference 5; we determined the divergence of the beam to be 316 mrad at the cathode.

The temporal pulse shape of the electron beam is modelled by adjusting the input particle distribution to closely match the shape the electron beam measured on the Faraday Cup located downstream of the gun, prior to the subharmonic buncher. The pulse shape is similar to a Gaussian with a long tail. Figure 2 shows a comparison of the measurement with the simulation output.

The electron gun was modelled in POISSON by the vendor. [1]

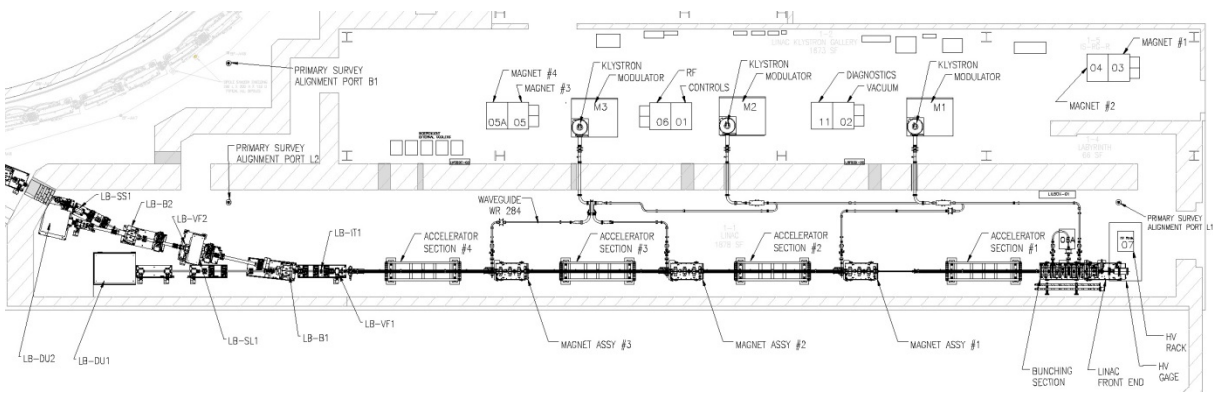

Figure 1: Layout of the NSLS-II linac along with the diagnostic transport line.

ISBN: 978-3-95450-132-8 doi:10.18429/JACoW-IPAC2014-WEPRO019

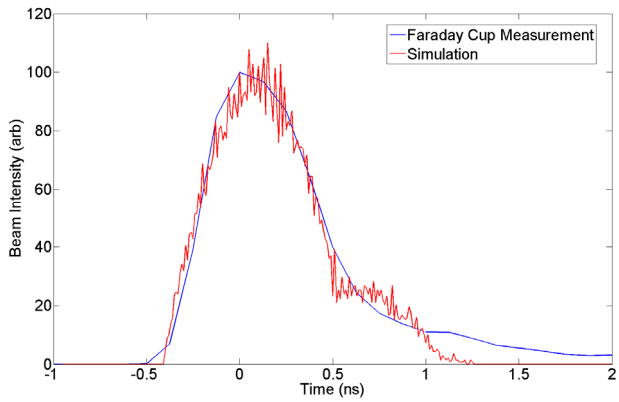

Figure 2: Comparison of the pulse shape of the beam in the simulation and measurement for single bunch mode.

There are three types of solenoids surrounding the linac in the first 2.8m for a total number of 20 solenoids. These solenoids are powered by 11 power supplies. The simulation models the solenoids using COIL elements. The current in the simulation is chosen to be the as run current with a small correction where needed to make the modelled field match the vendor supplied measurements. The first solenoid has a 1.2 mm offset and a 0.9 mrad angle relative to the beam trajectory. The remaining solenoids are aligned to less than 140 μm. The gun has a surveyed misalignment of 1 mm vertically and a 5 mrad upward angle. As mentioned above, these transverse offsets are not included in the model, but will be discussed later.

The field in the RF cavities is modelled based on the vendor supplied measurements of the gradient vs. cell number and the power that was measured at each cavity. A multipacting problem in the 3 GHz buncher meant that it could not be using during booster commissioning and therefore was not used in the simulations.

The phase of the cavities relative to the beam cannot be determined from measurements. Therefore the phases were selected in a two stage manner. In the first stage, a genetic optimization routine was used to select the phases of the subharmonic buncher and the buncher cavity. This was necessary as the dynamics of the beam in the bunching section is complicated by the non-relativistic velocity integral to the bunching process and space charge effects. The optimizer adjusted the RF phases until the number of particles outside an energy window of 1 MeV and a time window of 35 ps was minimized. In the second stage, the phases of the accelerating cavities were determined via phase scan of each individual cavity and maximizing the number of particles in the same energy time window.

Additional considerations are needed to simulate the linac in multiple bunch mode. First and foremost, beam loading is a large effect in the linac. Therefore a special model was produced to simulate the effect of beam loading in the NSLS-II linac and is presented in Reference 6.

The bunch train is not uniform in multiple bunch mode, as seen in Figure 3. Less obvious from the figure is that the bunch length is 30% shorter as compared to single bunch mode. The circuit used to generate the bunch train is multiple bunch mode is different than the circuit used in single bunch mode and accounts for these differences. The multiple bunch mode simulation uses the average charge per bunch and the width from the fit to the data.

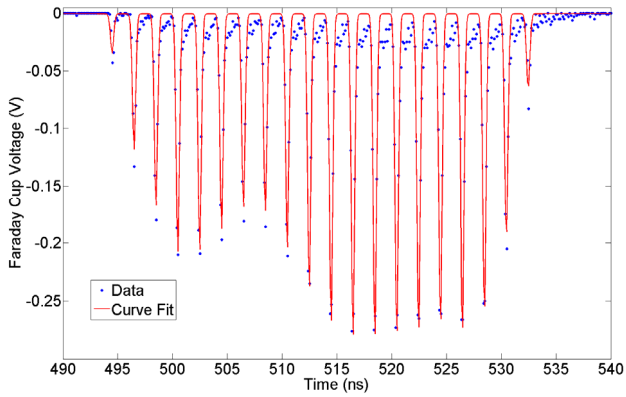

Figure 3: Typical 20 bunch train. The blue is the measurement and red is a curve fit to 20 Gaussians.

MEASUREMENTS

Measurements of the linac occurred routinely during booster and storage ring commissioning. Beam charge was monitored continuously using the wall current monitor after the linac gun and the integrating current transformer at the start of the transport line. A transport efficiency of 70% was routine. The model shows 100% efficiency. Energy and energy spread measurements were performed on a flag downstream of the first dipole magnet. The beam was horizontally focused on the flag to minimize beam size. The dispersion at the flag is 0.864 m, which dominates the beam size. During the multiple bunch mode measurements presented in this paper, beam loading compensation had not yet been commissioned in the linac. Transverse emittance is measured using a quadrupole scan in the straight diagnostic line onto an Optical Transition Radiation screen.

Table 1 contains a comparison of the simulations with measurements. There is very good agreement between the energy and the energy spread. The emittance in the simulations is 30% lower than the measurements, except for the vertical emittance in multiple bunch mode which is 2.4 times lower than the measured value.

The bunching section of the linac is completely contained within a solenoidal field. Prior to the buncher cavity, the beam is not relativistic. The subharmonic buncher provides a time dependent kick to the beam to accelerate the tail of the bunch and decelerate the head in order to compress the bunch. The induced momentum difference in the bunch is ± 18% with a similar change to the solenoidal focusing strength until the bunch is accelerated in the buncher and the relative momentum spread is decreased. This leads to emittance growth between the subharmonic prebuncher and the buncher. Longer bunch lengths from the gun will have increased emittance because of this. Figures 2 and 3 show that the

ISBN: 978-3-95450-132-8 doi:10.18429/JACoW-IPAC2014-WEPRO019

Table 1: Comparison of Models and Measurements in Single and Multiple Bunch Modes

Parameter	Single Bunch		Multiple Bunch	
	Simulation	Measurement	Simulation	Measurement
Bunch Charge after Gun (nC)	0.5	0.5	0.1	0.1 (averaged over 20 bunches)
Bunch Length (ns FWHM)	0.59	0.51±0.01	0.42	0.44±0.01
Energy (MeV)	198.3	200 ± 1	197.9	199 ± 1
Energy Spread (%)	0.1	0.16 ± 0.01	0.5	0.45 ± 0.3
ε_x (nm)	52	69 ± 3	31	47 ± 2
ε_y (nm)	92	126 ± 5	29	72 ± 3
σ_x (mm)	2.74	0.87 ± .01	2.81	No Measurement
σ_y (mm)	1.93	1.25 ± .01	1.78	No Measurement
X-Y coupling Angle	16	32 ± 1	15	No Measurement

bunch length is smaller in single bunch then in multiple bunch mode. This explains the smaller emittance in multiple bunch mode in both the measurements and the simulations.

Additionally, the misalignment of the gun and first solenoid serve to further increase the emittance. Calculations were performed to determine the expected increase in the emittance due to these misalignments. [7] These calculations only considered the section of the linac starting at the subharmonic prebuncher and ending at the start of the buncher cavity. These calculations show that with the present alignment, we can expect an emittance increase on the order of 20%. Factoring in this increase improves the agreement between the simulation and the measurement.

The beam exiting the linac exhibits an x-y coupling angle and unequal transverse emittances. [2] The beam is symmetric prior to the quadrupoles and coupling appears after the beam is focused in any quadrupole, therefore skewed quadrupoles can be ruled out. A magnetic field on the cathode of the gun will provide angular momentum to the beam which will generate this coupling and unequal emittances after the beam is passed through a quadrupole. [4] The remnant field of the linac solenoids at the cathode surface is 19 Gauss. Measurements taken at the cathode connector behind the gun were 21 Gauss. This alone did not produce the coupling in the simulation nor unequal emittances. As mentioned above, the cathode heater is a small solenoidal winding. The winding increases the field on the axis to approximately 46 Gauss. Furthermore, since the winding is smaller than the cathode emitting area, there is flux return on the edges of the cathode. This winding was added to the simulation and immediately the coupling was generated. The angle is half of that is predicted, which may be due to the focusing errors discussed in the next paragraph. This coupling can be removed in the future by either pulsing the heater supply off during the beam pulse or driving the heater AC.

One area where the model does not reproduce the data well is the twiss functions and beam sizes along the linac. The linac is equipped with 6 flags for beam imaging. The first flag is 53 cm from the cathode, prior to the prebunching cavity. The beam size is 3 mm on this flag, and the simulation predicts 1.5 mm. The only components upstream of this flag are the gun and the first solenoid. The first solenoid has not been measured, and may be different then the model or the gun model may not be accurate.

CONCLUSION

A model of the NSLS-II linac has been presented. This model reflects the as built and as run conditions of the linac. Comparisons of the model to measurements show that the energy and energy spread are predicted with good accuracy. The predicted emittance is smaller than what has been observed. Calculations show that misalignments of the gun and solenoids in the bunching section can drive the emittance higher by 20% which improves the agreement with observations. The observed coupling and unequal emittances can be explained by considering the magnetic field produced by the cathode heater. The predicted twiss functions do not match the observed functions. This has been traced to a difference originating in the bunching section of the linac, but is not fully explained.

REFERENCES

[1] K. Dunkel. 200 MeV Linac for NSLS-II/Beam dynamics report for FDR. RI report Number 3200-BP-8531-A.

[2] R. Fliller III et al., "Results of NSLS-II Linac Commissioning", WEPWA083, International Particles Accelerator Conference 2013, Shanghai, China.

[3] Ricky Ho. Communications and Power Industries. Private Communication.

[4] Y.-E.Sun, P. Piot, K.-J. Kim, N. Barov, S. Lidia, J. Santucci, R. Tikhoplav, J. Wennerberg. Phys. Rev. ST Accel. Beams 7, 123501 (2004).

[5] Y. Zou, H. Li, M. Reiser, P.G. O'Shea. Nucl. Inst. And Meth. A 519 (2004) 432-441.

[6] R. Fliller III et al. "Theoretical Maximum Current of the NSLS-II Linac", IPAC14, these proceedings.

[7] R. Fliller III. Unpublished.